Efficient calculation of Rayleigh and Raman scattering

K. McNamara,* D. V. Fursa, and I. Bray

Curtin Institute for Computation and Department of Physics, Astronomy and Medical Radiation Sciences, Curtin University, Perth, Western Australia 6102, Australia

(Received 11 August 2018; published 30 October 2018)

We present two methods for computing the Rayleigh and Raman scattering cross sections for photon scattering on atomic hydrogen or hydrogenlike systems. Both methods are applicable for incident photon energies above the ionization threshold. The first method implements the well-known Gaussian quadrature approach to deal with principal value integration and relies on evaluation of the exact eigenfunctions of hydrogen. The second, more computationally efficient approach uses a finite-L^2 basis expansion of the target and applies complex exterior scaling methods to accurately account for the contribution of the intermediate continuum states. This method is much more general in that it does not rely on analytic solutions to the Hamiltonian, or evaluation of any special functions, and is expected to be applicable to more complex systems where exact wave functions are cumbersome to evaluate. Both methods are in complete agreement with previous work based on analytical representations of the Green's function or the dipole matrix elements. Rayleigh, Raman, and photoionization cross sections for scattering on the first few excited states of atomic hydrogen are presented and compared with previous results where available.

DOI: 10.1103/PhysRevA.98.043435

I. INTRODUCTION

The problem of photon-atom scattering using a fully quantum approach has been well understood since the mid 1920s. The development of the Kramers-Heisenberg-Waller (KHW) matrix elements [1–3] provided a clear description of photon scattering processes up to second order in perturbation theory. In turn, it established the foundation for various applications of photon scattering processes, such as Raman spectroscopy [4], radiation transport and opacity [5,6], and, more recently, quantum illumination and radars [7,8].

Calculation of the KHW matrix elements is complicated by contributions from the continuum and, for incident photon energies above the ionization threshold, the need to correctly deal with the pole terms. Most calculations are restricted to the case where the Green's function may be given analytically or where the bound-bound and bound-free dipole matrix elements are known analytically. For example, Gavrila [9] presented analytical expressions for the elastic scattering of photons from the ground state. Saslow and Mills [10] presented analytic expressions for the $1s \rightarrow 2s$ Raman scattering transitions and discussed the importance of the continuum intermediate states. Sadeghpour and Dalgarno [11] calculated Rayleigh and Raman scattering by hydrogen and cesium using numerical solutions to the response functions to avoid the infinite summation in the KHW matrix elements. Many other publications which consider Rayleigh and Raman scattering restrict their calculations to below the ionization threshold. For example Drühl [12] considered Raman scattering on iodine using only small incident photon energies and was, thus, able to approximate a sum over all intermediate states using dipole summation rules. Delserieys *et al.*[13] considered Raman scattering on Mg using only contributions from a small number of bound states and assumed that contributions from all other states are negligible.

A recent publication by Bachau *et al.* [14] considered scattering of short laser pulses on the metastable $2s$ state of hydrogen and showed that for the intensity considered (3.51×10^{16} W cm^{-2}), results from solving the time-dependent Schrödinger equation were in good agreement with the KHW matrix element calculation using perturbation theory. In order to calculate the KHW matrix element they considered two analytic approaches, the first requiring the evaluation of Appell functions and the second using an inhomogeneous differential-equation-type method. This is in contrast to the relative simplicity of the equations for scattering from the $1s$ state [15] and shows that the complexity of the analytic forms grows when considering scattering from higher excited states.

Here we present two computational approaches for scattering of photons on hydrogen atoms at low and intermediate incident energies. These techniques do not rely on analytical evaluation of the Green's function or the dipole matrix elements. The first method provides a direct numerical calculation of the KHW matrix element for particular transitions using the exact eigenfunctions to calculate the dipole matrix elements. The second method uses a finite L^2 basis and complex exterior scaling (CES) [16–18] to accurately account for contributions from all intermediate states and provides a computationally efficient and accurate method for calculating the KHW matrix element for transitions between any two states at arbitrary photon energies.

II. THEORY

A. Photon-atom scattering

In this paper we use atomic units. The nonrelativistic atom-field interaction Hamiltonian is written in the Coulomb

*Keegan.McNamara@curtin.edu.au

gauge as

$$H_{\rm int} = \frac{\mathbf{A}^2}{2c^2} - \frac{\mathbf{A}\cdot\mathbf{p}}{c}. \tag{1}$$

By considering only the first-order contributions of the seagull term, $\mathbf{A}^2$, and second-order contributions of the $\mathbf{A}\cdot\mathbf{p}$ term, the differential cross section for photon scattering between two states is given by

$$\frac{d\sigma_{fi}}{d\Omega} = r_0^2 \frac{\omega'}{\omega} |M_{fi}|^2, \tag{2}$$

where r_0 is the classical electron radius, and ω and ω' denote the energy of the incident and outgoing photons. M_{fi} is the well-known Kramers-Heisenberg-Waller matrix element [1,2],

$$\begin{aligned} M_{fi} =& \boldsymbol{\epsilon}\cdot\boldsymbol{\epsilon}'^{*}\langle f|e^{i(\mathbf{k}-\mathbf{k}')\cdot\mathbf{r}}|i\rangle \\ &- \sum\!\!\!\!\!\!\int_t \left[\frac{\langle f|e^{-i\mathbf{k}'\cdot\mathbf{r}}(\boldsymbol{\epsilon}'^{*}\cdot\mathbf{p})|t\rangle\langle t|e^{i\mathbf{k}\cdot\mathbf{r}}(\boldsymbol{\epsilon}\cdot\mathbf{p})|i\rangle}{E_t - E_i - \omega - i0}\right. \\ &\left. + \frac{\langle f|e^{i\mathbf{k}\cdot\mathbf{r}}(\boldsymbol{\epsilon}\cdot\mathbf{p})|t\rangle\langle t|e^{-i\mathbf{k}'\cdot\mathbf{r}}(\boldsymbol{\epsilon}'^{*}\cdot\mathbf{p})|i\rangle}{E_t - E_i + \omega'}\right], \end{aligned} \tag{3}$$

where $\boldsymbol{\epsilon}$ ($\boldsymbol{\epsilon}'$) and $\mathbf{k}$ ($\mathbf{k}'$) denote the incident (outgoing) photon polarization and momenta, respectively, E_t denotes the energy of state $|t\rangle$, and the sum represents a sum over all intermediate bound states as well as an integral over the continuum. The outgoing photons satisfy the energy conservation condition $E_i + \omega = E_f + \omega'$. As we are considering Rayleigh and Raman scattering to low-lying (i.e., not Rydberg) states, it is reasonable and convenient to apply the dipole approximation, equivalent to setting $\mathbf{k} = \mathbf{k}' = 0$. We also limit our calculations to relatively low photon energies, $\omega < 10$ a.u., where the $\mathbf{A}\cdot\mathbf{p}$ terms are dominant [15]. Using the dipole approximation the KHW matrix element may be rewritten as

$$\begin{aligned} M_{fi} =& \omega\omega' \sum\!\!\!\!\!\!\int_t \left[\frac{\langle f|\boldsymbol{\epsilon}'^{*}\cdot\mathbf{D}|t\rangle\langle t|\boldsymbol{\epsilon}\cdot\mathbf{D}|i\rangle}{E_t - E_i - \omega - i0}\right. \\ &\left. + \frac{\langle f|\boldsymbol{\epsilon}\cdot\mathbf{D}|t\rangle\langle t|\boldsymbol{\epsilon}'^{*}\cdot\mathbf{D}|i\rangle}{E_t - E_i + \omega'}\right], \end{aligned} \tag{4}$$

where $\mathbf{D}$ is the length form of the dipole operator. It has been shown that the scattering matrix for nonoriented systems, i.e., those in which the initial magnetic sublevels are averaged and the final magnetic sublevels are summed over, may be written as a sum of irreducible tensor components [12,19]. We use the notation of Delserieys *et al.* [13] and write the scattering cross section for a nonoriented target as

$$\begin{aligned} \frac{d\sigma_{n'l'nl}}{d\Omega} =& r_0^2 \frac{\omega\omega'^3}{3}\frac{1}{2l+1}\left[\left|A^{(0)}_{n'l'nl}\right|^2 |\boldsymbol{\epsilon}'^{*}\cdot\boldsymbol{\epsilon}|^2\right. \\ &+ \frac{3}{2}\left|A^{(1)}_{n'l'nl}\right|^2 (1 - |\boldsymbol{\epsilon}'\cdot\boldsymbol{\epsilon}|^2) + \frac{3}{2}\left|A^{(2)}_{n'l'nl}\right|^2 \\ &\left.\times\left(1 + |\boldsymbol{\epsilon}'\cdot\boldsymbol{\epsilon}|^2 - \frac{2}{3}|\boldsymbol{\epsilon}'^{*}\cdot\boldsymbol{\epsilon}|^2\right)\right], \end{aligned} \tag{5}$$

which implicitly depends on photon polarization $\boldsymbol{\epsilon}$ ($\boldsymbol{\epsilon}'$). In what follows we use the compound notations $|i\rangle \equiv |nlm\rangle$, $|f\rangle \equiv |n'l'm'\rangle$, $|t\rangle \equiv |n_t l_t m_t\rangle$, where n stands for the principal quantum number, l for the orbital angular momentum, and m for its projection. The tensor expansion coefficients $A^{(\kappa)}_{n'l'nl}$ are given by

$$\begin{aligned} A^{(\kappa)}_{n'l'nl} =& (-1)^{l+l'+\kappa} \sum\!\!\!\!\!\!\int_t \begin{Bmatrix} l & l' & \kappa \\ 1 & 1 & l_t \end{Bmatrix} \langle n'l'\|D\|n_t l_t\rangle\langle n_t l_t\|D\|nl\rangle \\ &\times\left[\frac{1}{E_{n_t l_t} - E_{nl} - \omega - i0} + \frac{(-1)^\kappa}{E_{n_t l_t} - E_{nl} + \omega'}\right], \end{aligned} \tag{6}$$

where $\langle \ldots \|D\| \ldots\rangle$ are reduced matrix elements [20]. If we are not interested in the polarization of the photons, we may sum over the final polarizations and average over the initial polarization to give the unpolarized scattering cross section,

$$\begin{aligned} \frac{d\sigma_{n'l'nl}}{d\Omega} =& r_0^2 \frac{\omega\omega'^3}{6}\frac{1}{2l+1}\left[\left|A^{(0)}_{n'l'nl}\right|^2 (1 + \cos^2\theta)\right. \\ &+ \frac{3}{2}\left|A^{(1)}_{n'l'nl}\right|^2 (2 + \sin^2\theta) \\ &\left.+ \left|A^{(2)}_{n'l'nl}\right|^2 \left(\frac{13}{2} + \frac{1}{2}\cos^2\theta\right)\right], \end{aligned} \tag{7}$$

where θ denotes the scattering angle. Integrating over all solid angles $d\Omega$ gives the total integrated cross section for Raman or Rayleigh scattering,

$$\sigma_{n'l'nl} = \sigma_T \frac{\omega\omega'^3}{3(2l+1)} \sum_\kappa (2\kappa+1)\left|A^{(\kappa)}_{n'l'nl}\right|^2, \tag{8}$$

where $\sigma_T = 8\pi r_0^2/3 \approx 6.652 \times 10^{-29}$ m^2 is the Thompson cross section. As in [13] the $\kappa = 0$ component is proportional to the polarizability,

$$A^{(0)}_{nlnl} = \sqrt{3(2l+1)}\alpha_{nl}(\omega), \tag{9}$$

which allows for calculation of the total photoionization cross section,

$$\sigma^l_{nl} = \frac{1}{2}\sigma_T c^3 \omega\, {\rm Im}\left\{A^{(0)*}_{nlnl}\right\}\sqrt{\frac{3}{2l+1}}. \tag{10}$$

In Appendix B we show how the scattering cross sections may be calculated in the velocity gauge.

B. Resonance behavior

In Eq. (3), and those which follow from it, it is clear that the KHW matrix element becomes infinite when the quantity $\Delta_a = E_t - E_i - \omega$ or $\Delta_e = E_t - E_i + \omega'$ becomes 0. If $|t\rangle$ is a continuum state, then this is formally handled through contour integration around the singular point, and no unphysical results arise. If, however, $|t\rangle$ is a bound state, then unphysical resonances occur due to the neglect of the finite lifetimes of the states [3,21]. In Fig. 1 we schematically show how these processes occur. One standard approach to calculation of the KHW matrix elements at or near these singularities involves the introduction of a complex damping term [3], which can be achieved through the substitution $E_t \to E_t - i\Gamma_t/2$, where Γ_t is the linewidth of state $|t\rangle$. Wijers [22] has argued that the introduced terms should in fact be frequency dependent to ensure that the damping term goes to 0 as $\omega \to 0$. For multiphoton processes where resonances occur the method of

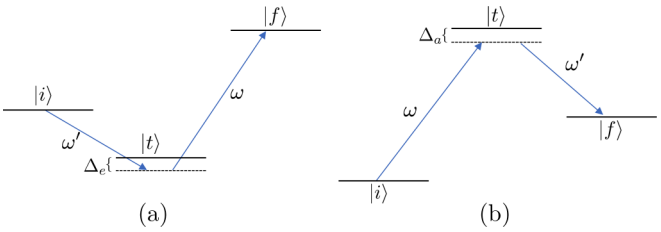

FIG. 1. Schematic of the resonant processes in photon scattering. (a) The emission-then-absorption term is resonant if the detuning Δ_e, defined by $\Delta_e = E_t - E_i + \omega'$, is small. (b) The absorption-then-emission term is resonant if the detuning Δ_a, defined by $\Delta_a = E_t - E_i - \omega$, is small, and $|t\rangle$ is a bound intermediate state.

resolvent equations is also often applied [23]. Presently, we choose not to explicitly deal with resonant behavior, as we are more interested in demonstrating the capabilities of the methods. This allows us to directly compare our calculations with previously published analytical results.

III. CALCULATION METHODS

In this section we outline two computational methods for calculating Rayleigh and Raman scattering. In Sec. III A we present an approach which calculates the KHW matrix elements for particular transitions and incident photon energies by generating a suitable set of true hydrogen eigenfunctions. In Sec. III B we present a new method for calculation of Rayleigh and Raman cross sections using CES [18].

A. Principal value approach

The first method we consider for calculating the cross section is a straightforward explicit calculation of the matrix elements using the true bound and continuum eigenstates of hydrogen; we refer to this method throughout the text as the principal value (PV) method. The sum in Eq. (6) is broken into a sum over bound states, a PV integral over the continuum, and an imaginary contribution from the pole term,

$$A^{(\kappa)}_{n'l'nl} = (-1)^{l+l'+\kappa} \sum_{l_t} \begin{Bmatrix} l & l' & \kappa \\ 1 & 1 & l_t \end{Bmatrix} \Bigg(\sum_{n_t=l_t+1}^{N_b} \langle n'l' \| D \| n_t l_t \rangle \langle n_t l_t \| D \| nl \rangle \left[\frac{1}{E_{n_t l_t} - E_{nl} - \omega} + \frac{(-1)^\kappa}{E_{n_t l_t} - E_{nl} + \omega'} \right]$$
$$+ \mathrm{P} \int dE \, \frac{\langle n'l' \| D \| E l_t \rangle \langle E l_t \| D \| nl \rangle}{E - E_{nl} - \omega} + i\pi \langle n'l' \| D \| (E_{nl} + \omega) l_t \rangle \langle (E_{nl} + \omega) l_t \| D \| nl \rangle$$
$$+ (-1)^\kappa \int dE \, \frac{\langle n'l' \| D \| E l_t \rangle \langle E l_t \| D \| nl \rangle}{E - E_{nl} + \omega'} \Bigg). \tag{11}$$

Here the states $|n_t l_t\rangle$ refer to the bound states, while $|E l_t\rangle$ refer to continuum states of energy E. Formally $N_b = \infty$, however, practically we may choose sufficiently large N_b so that the sum converges. If the incident photon energy is such that $E_{nl} + \omega < 0$, then the imaginary part of the second line of Eq. (11) is ignored, and the PV integral reduces to a regular integral. When $E_{nl} + \omega > 0$ the principal value integral is calculated using the Gaussian quadrature approach outlined by Bray and Stelbovics [24], which has been applied to a large variety of collision problems involving electrons and positrons scattering from atoms, ions, and molecules [25,26]. This approach provides a clear representation of the problem and allows us to test the convergence of our results by increasing the number of bound states included and the number of points in the quadrature. The method, however, is computationally inefficient, as the quadrature chosen depends on the location of the singularity, which is fixed by both the energy of the initial state and the energy of the incident photon. Thus in order to calculate the energy-dependent scattering cross section we are required to calculate a new quadrature for each photon energy (above the ionization threshold) and must also calculate the continuum wave functions at these new points. The procedure outlined in this section also relies on the ability to obtain, either numerically or analytically, the exact wave functions for the target. This is not easily generalizable to more complex systems, particularly in the case of the continuum wave functions.

B. Complex exterior scaling method

In this section we present a new approach to calculation of the photon scattering matrix. This approach was inspired by the work of Rescigno and McKoy [18], who used the complex rotation method (commonly referred to as the complex scaling method or complex exterior scaling) in order to calculate the photoionization cross section for hydrogen. Their approach has many enticing benefits, such as the use of a finite-L^2 basis, the simplicity with which the contribution from the pole term is accounted for, and the capability for calculations over a broad range of incident photon energies. Finite-L^2 methods are also more easily generalizable to complex systems such as atoms and molecules (see, for example, Han and Yarkony [27]). Throughout we refer to this as the complex exterior scaling method. To outline the method we first consider the simpler problem of calculating the sum

$$\sum_t \!\!\!\!\!\!\int \frac{\langle n'l'm' | D_\rho | n_t l_t m_t \rangle \langle n_t l_t m_t | D_\sigma | nlm \rangle}{E_{n_t l_t} - E_{nl} - \omega - i0}, \tag{12}$$

where D_ρ is the ρth component of the dipole operator, and we find it convenient to use spherical basis vectors so that D_ρ is an irreducible tensor of rank 1. If we choose to use finite-L^2 methods, then the sum and integral over all intermediate states are approximated by a sum over pseudostates. For incident photon energies above the ionization threshold such methods would contain unphysical singularities [18]. Following the

approach of Rescigno and McKoy we rewrite the sum as

$$\langle n'l'm'|D_\rho \frac{1}{H-E_{nl}-\omega} D_\sigma |nlm\rangle = \int d^3\mathbf{r}\, \psi^*_{n'l'm'}(\mathbf{r}) D_\rho(\mathbf{r}) \frac{1}{H(\mathbf{r})-E_{nl}-\omega} D_\sigma(\mathbf{r}) \psi_{nlm}(\mathbf{r}), \tag{13}$$

where H is the Hamiltonian of the atom. Here we are considering scattering from hydrogen, so that the wave functions ψ may be written as

$$\psi_{nlm}(\mathbf{r}) = \frac{1}{r} u_{nl}(r) Y_l^m(\hat{\mathbf{r}}). \tag{14}$$

We then analytically continue the radial coordinates of the Hamiltonian by taking $r \to r\theta$, where $\theta = e^{i\varphi}$ and $0 < \varphi < \pi/2$. This leads to

$$\theta^3 \int d^3\mathbf{r}\, \psi^\dagger_{n'l'm'}(\mathbf{r}\theta) D_\rho(\mathbf{r}\theta) \frac{1}{H_\theta - E_{nl} - \omega} D_\sigma(\mathbf{r}\theta) \psi_{nlm}(\mathbf{r}\theta), \tag{15}$$

where $H_\theta \equiv H(\mathbf{r}\theta)$, and the dagger indicates complex conjugation of the angular components of the wave-function but not of the radial component. The properties of such analytically continued Hamiltonians have been described in the fundamental work by Balslev and Combes [16], as well as Simon [17], and have typically been used to study resonances in atoms and molecules [28]. In performing the CES we require that the initial and final states of the system decrease sufficiently rapidly at ∞, especially under analytic continuation. Following the procedure of Rescigno and McKoy [18] we wish to diagonalize the complex symmetric Hamiltonian H_θ in a finite-L^2 basis. Here we choose the radial Laguerre functions, used commonly in the convergent close-coupling formalism [25,26],

$$\xi_{kl}(r) = \sqrt{\frac{\alpha_l (k-1)!}{(k+l)(k+2l)!}} (2\alpha_l r)^{l+1} \exp(-\alpha_l r) L_{k-1}^{2l+1}(2\alpha_l r), \tag{16}$$

where L_k^n are the associated Laguerre polynomials. Under complex exterior scaling the atomic Hamiltonian H, provided that the potentials are Coulombic, transforms as

$$H = K + V \to H_\theta = \theta^{*2} K + \theta^* V. \tag{17}$$

As the matrix elements $\langle \xi_{kl}|K|\xi_{k'l}\rangle$ and $\langle \xi_{kl}|V|\xi_{k'l}\rangle$ are known analytically, it is simple to extend these results to calculation of the matrix elements $\langle \xi_{kl}|H_\theta|\xi_{k'l}\rangle$. We then diagonalize the complex symmetric matrix to find pseudostates, which are written as a sum over the nonrotated basis functions,

$$\chi^\theta_{nlm}(\mathbf{r}) = \frac{1}{r} v^\theta_{nl}(r) Y_l^m(\hat{\mathbf{r}}), \quad v^\theta_{nl}(r) = \sum_k a_{nk} \xi_{kl}(r), \tag{18}$$

where the a_{nk} are complex numbers found in the diagonalization process, and the superscript θ denotes that the states are pseudostates of the complex exterior scaled Hamiltonian. The pseudostates satisfy

$$(\chi^\theta_{nlm}|H_\theta|\chi^\theta_{n'l'm'}) = W_{nl}(\chi^\theta_{nlm}|\chi^\theta_{n'l'm'}), \tag{19}$$

where we use the c norm described by Moiseyev *et al.* [28], given by

$$(\chi^\theta_{nlm}|\chi^\theta_{n'l'm'}) = \int d^3\mathbf{r}\, \chi^{\theta\dagger}_{nlm}(\mathbf{r}) \chi^\theta_{n'l'm'}(\mathbf{r}), \tag{20}$$

and W_{nl} are the complex eigenvalues. Giraud and Katō [29] provided a proof of the completeness of complex scaled Hamiltonians, however, Moiseyev *et al.* [28] noted that incompleteness pathologies may still arise when performing finite basis calculations. As a precaution, within our code we check that all pseudostates are indeed c-normalizable, allowing us to approximate the Green's function using the sum over all pseudostates. We are now able to write the sum, (12), as

$$\theta^3 \sum_t \frac{\int d^3\mathbf{r}\, \psi^\dagger_{n'l'm'}(\mathbf{r}\theta) D_\rho(\mathbf{r}\theta) \chi^\theta_{n_t l_t m_t}(\mathbf{r}) \int d^3\mathbf{r}\, \chi^{\theta\dagger}_{n_t l_t m_t}(\mathbf{r}) D_\sigma(\mathbf{r}\theta) \psi_{nlm}(\mathbf{r}\theta)}{W_{n_t l_t} - E_{nl} - \omega}. \tag{21}$$

The procedure described above was used by Rescigno and McKoy [18] in the case where the initial and final states were the ground state of hydrogen, and only the z component of the dipole operators was considered. The generality of our consideration now allows us to apply the Wigner-Eckart theorem to the angular components of the above; noting that only the radial part of the calculation has been altered by the complex scaling, we may write

$$(\psi_{nlm}|D_\rho|\chi^\theta_{n_t l_t m_t})_\theta \equiv \int d^3\mathbf{r}\, \psi^\dagger_{nlm}(\mathbf{r}\theta) D_\rho(\mathbf{r}\theta) \chi^\theta_{n_t l_t m_t}(\mathbf{r}) = (-1)^{l-m} \begin{pmatrix} l & 1 & l_t \\ -m & \rho & m_t \end{pmatrix} \left(\psi_{nl} \| D \| \chi^\theta_{n_t l_t}\right)_\theta. \tag{22}$$

We note that the inner product defined above makes a distinction between the state on the left, which is an eigenstate of the real Hamiltonian, and the state on the right, which is an eigenstate of the complex exterior scaled Hamiltonian. The reduced matrix elements of this inner product are given by

$$\left(\psi_{nl} \| D \| \chi^\theta_{n_t l_t}\right)_\theta = (-1)^l \sqrt{(2l+1)(2l_t+1)} \begin{pmatrix} l & 1 & l_t \\ 0 & 0 & 0 \end{pmatrix} \int dr\, u_{nl}(r\theta) r\theta v^\theta_{n_t l_t}(r). \tag{23}$$

The same arguments presented in [12], [13], and [19] then allow the scattering cross section to be written exactly as in Eq. (5), where now the $A^{(\kappa)}_{n'l'nl}$ are defined as

$$A^{(\kappa)}_{n'l'nl} = \theta(-1)^{l+\kappa} \sum_t \begin{Bmatrix} l & l' & \kappa \\ 1 & 1 & l_t \end{Bmatrix} \left(\psi_{n'l'} \| D \| \chi^{\theta}_{n_t l_t}\right)_\theta \left(\psi_{nl} \| D \| \chi^{\theta}_{n_t l_t}\right)_\theta \left[\frac{1}{W_{n_t l_t} - E_{nl} - \omega} + \frac{(-1)^\kappa}{W_{n_t l_t} - E_{nl} + \omega'}\right]. \tag{24}$$

The sum is now a finite sum over the complex rotated pseudostates and converges to Eq. (6) as the basis size increases. Using Eqs. (9) and (10) we recover the results of Rescigno and McKoy and generalize it to the case where the ground state (or excited state of interest) is not an s state.

As an interesting additional result we consider the imaginary part of the $\kappa = 0$ component of Eq. (6) and note that this directly relates to the bound-free matrix elements. To exploit this we define a new quantity for the case of elastic scattering on a state nl, where we sum only over the subspace of intermediate states of fixed l_t,

$$A^{l_t}_{nl}(E) = (-1)^{l_t - l} \sum\!\!\!\!\!\!\int_{n_t} \frac{\langle nl \| D \| n_t l_t \rangle \langle n_t l_t \| D \| nl \rangle}{E_{n_t l_t} - E - i0}. \tag{25}$$

We find that the imaginary part of this quantity is

$$\mathrm{Im}\left\{A^{l_t}_{nl}(E)\right\} = \pi |\langle nl \| D \| E l_t \rangle|^2. \tag{26}$$

Similarly to Eq. (24) we may now calculate the sum and integral over all intermediate states using complex exterior scaled pseudostates, giving

$$A^{l_t}_{nl}(E) = \theta \sum_{n_t} \frac{\left(\psi_{nl} \| D \| \chi^{\theta}_{n_t l_t}\right)^2_\theta}{W_{n_t l_t} - E}, \tag{27}$$

which will converge to Eq. (25) as the basis size increases. As the Laguerre functions approximate a complete set of intermediate states for the subspace of each value of angular momentum, Eq. (27) provides an accurate method for calculation of Eq. (26) from any initial state and allows calculation of the bound-free matrix elements without the need for explicit calculation of the true continuum state.

We now also make note of the form of the complex scaled initial and final states. We may obtain $u_{nl}(r\theta)$ and $u_{n'l'}(r\theta)$ either from complex scaling of the analytical solutions to H or from coefficients obtained by diagonalizing the real Hamiltonian H using basis functions $\xi_{kl}(r)$ and then applying the complex scaling to the basis functions. We choose to apply the second method, as it is more likely to generalize to complex atoms and provides very little computation overhead. The intermediate states may only be obtained by diagonalization of the complex rotated Hamiltonian H_θ using real basis functions, which is done using the LAPACK routine zggev [30].

In Appendix C we show the velocity form of the CES method, allowing for comparison of the length and velocity forms of the scattering cross sections.

IV. RESULTS

Due to the versatility of the CES method we are able to generate scattering cross sections for transitions between any low-lying states of interest for incident photons at essentially any energy. We present scattering cross sections for Rayleigh and Raman scattering from the ground state and the first few excited states to demonstrate, then compare them to several analytic results. It is also possible to calculate differential cross sections for any particular transition at any given energy using Eq. (5) or (7). We find it more interesting to demonstrate the energy dependence of the integrated cross sections. All results are presented for the length gauge formulation, however, we have verified the results using the velocity gauge and found full agreement.

For calculations using the PV method we found that for transitions from the $1s$, $2s$, and $3s$ states it was sufficient to include $N_b = 40$ bound states. However, for other calculations, such as the $3p \rightarrow 2p$ Raman transitions (which include contributions from the intermediate d states), up to 100 bound-state functions were required for convergence. The positive energy spectrum used for the integration was dependent on the particular transition and incident energies. For calculations using the CES method we chose to use $N_l = 125 - l$ Laguerre functions for each angular momentum l and α_l values of 0.65 and 0.645 for $l = 0$ and 1, respectively. If higher-angular-momentum intermediate states were required, e.g., in $1s \rightarrow 3d$ transitions, we chose $\alpha_l = 0.64$ for $l > 1$. We also chose the angle of complex rotation to be 15°. A number of other choices were made to test the convergence of our results, and we found that the scattering cross sections converged quickly for all transitions and photon energies. Near the ionization threshold the cross sections are less accurate, as the pseudostates in that region do not accurately represent highly excited target states. In such regions resonance effects become more important and the inaccuracy of our results near these points is irrelevant.

In Fig. 2 we present our calculations for Rayleigh scattering on the ground state of hydrogen using both the CES and the PV methods. We compare our results with those of Gavrila [9], and find perfect agreement at all given energies.

In Fig. 3 we present the $2p$ Rayleigh scattering cross section, again finding excellent agreement between our two computational methods. We also make note of the resonant behavior which occurs above the ionization energy. This resonance corresponds to decay to the $1s$ state and is outlined in Fig. 1(a).

In Figs. 4 and 5 we present the Raman cross sections for scattering on the $1s$ and $3p$ states. The total Raman cross section has been calculated by summing contributions from the first 10 scattering states allowed by the dipole selection rules and is convergent to better than 1%. We have compared our $1s \rightarrow 2s$ results with analytic results of Saslow and Mills [10] (as discussed in Appendix A) and have found excellent agreement. We do not present the results of Saslow and Mills [10] in Fig. 4, as they are indistinguishable from our own.

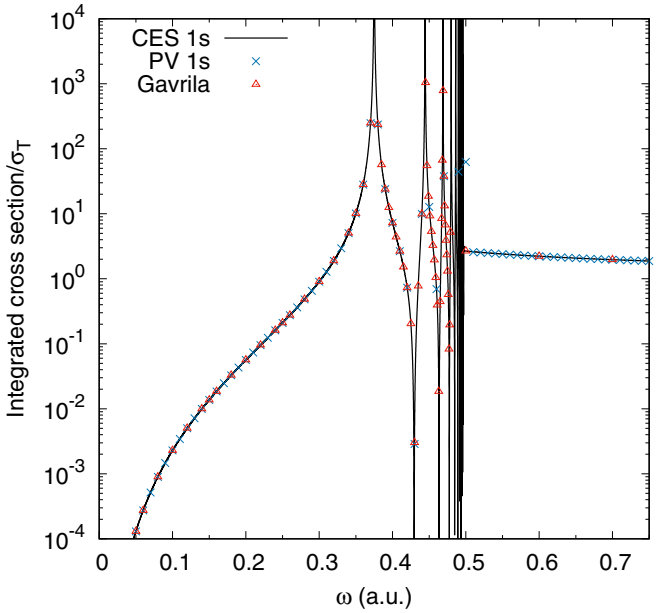

FIG. 2. Rayleigh scattering from the ground state of hydrogen calculated using the present CES and PV methods. Comparison is made of the elastic $1s$ results vs those of Gavrila [9]

In Fig. 5 we make note of the large cross section which occurs at low incident photon energies in the $3p \rightarrow 2p$ transition. If we consider the length form of the scattering tensor, (6), we see that the large cross section at low energies corresponds to absorption-type resonances [see Fig. 1(b)], with the intermediate $3s$ or $3d$ states of equal energy. If we instead consider the velocity form of the scattering cross sections, where the $3p \rightarrow 3s$ and $3p \rightarrow 3d$ momentum matrix elements are 0, the behavior is instead attributed to the ω'/ω prefactor of Eq. (B2).

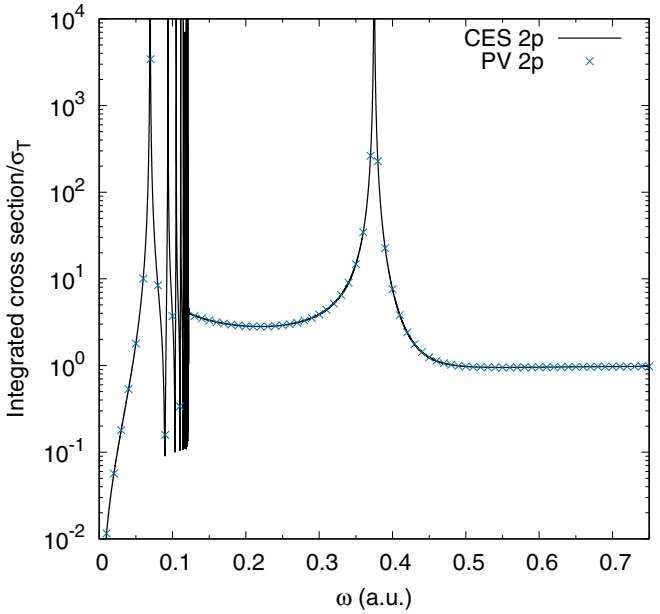

FIG. 3. Rayleigh scattering from the $2p$ state of hydrogen calculated using the CES and PV methods.

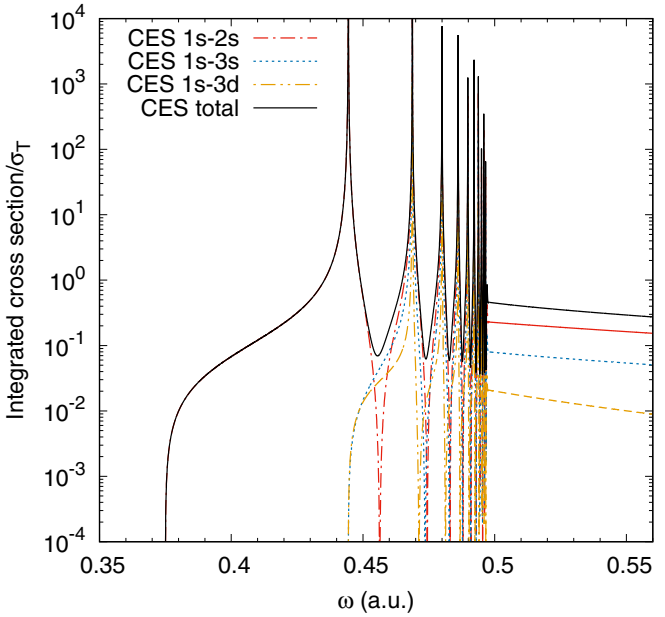

FIG. 4. Raman scattering from the $1s$ state. Our results for the $1s \rightarrow 2s$ transition are indistinguishable from analytic results of Saslow and Mills [10], which are omitted for clarity.

The total $3p$ Raman cross section shows two series of resonances above the ionization threshold. The first, occurring in the range $0.09 < \omega < 0.13$, corresponds to resonant processes involving the intermediate $2s$ state, while the second, occurring in the range $0.3 < \omega < 0.5$, corresponds to processes involving the intermediate $1s$ state. All resonant processes above the ionization energy correspond to emission-type resonances as shown in Fig. 1(a). We also show an example of a Raman transition between a p and an f state, which we have not found elsewhere in the literature.

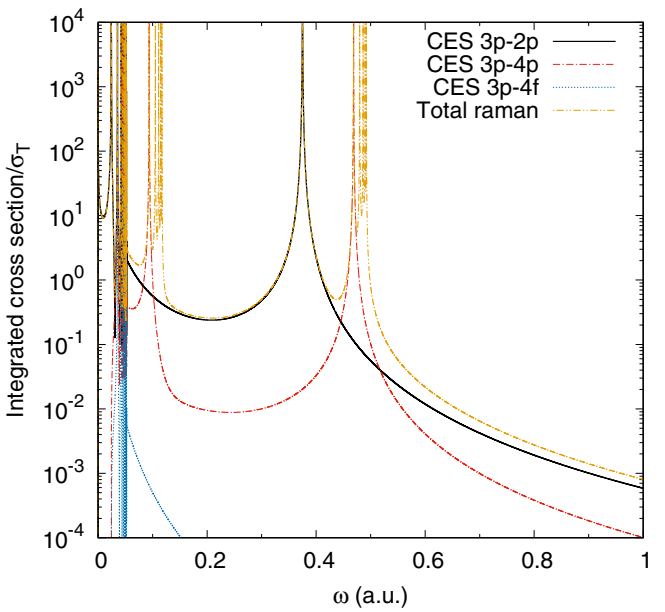

FIG. 5. Raman scattering from the $3p$ state.

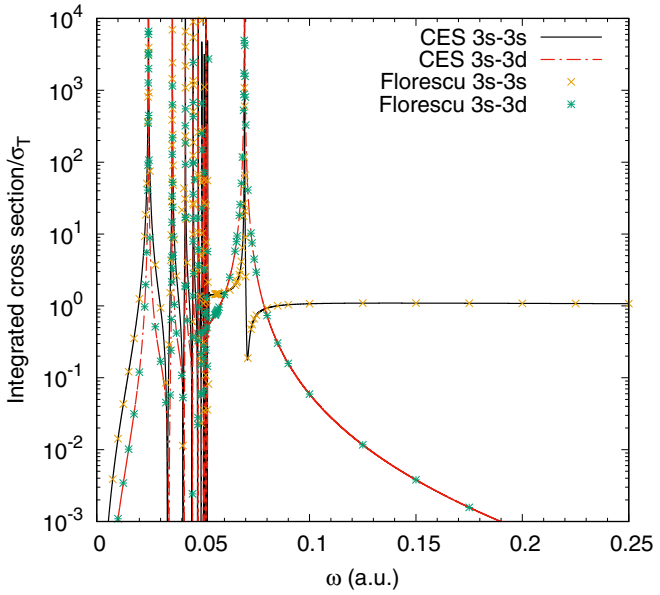

FIG. 6. Elastic scattering from the $3s$ state, with a comparison to the analytic calculations of Florescu and Cionga [31].

In Fig. 6 we present the cross sections for elastic scattering from the $3s$ state. We present both coherent ($3s \rightarrow 3s$) and incoherent ($3s \rightarrow 3d$) cross sections and compare with the analytic results of Florescu and Cionga [31], again showing excellent agreement with the analytic results.

In Fig. 7 we present the (one-photon) photoionization cross sections for ionization from the first five bound states of hydrogen. As in [18] we find that only a small number of pseudostates are required for convergence of the photoionization cross section.

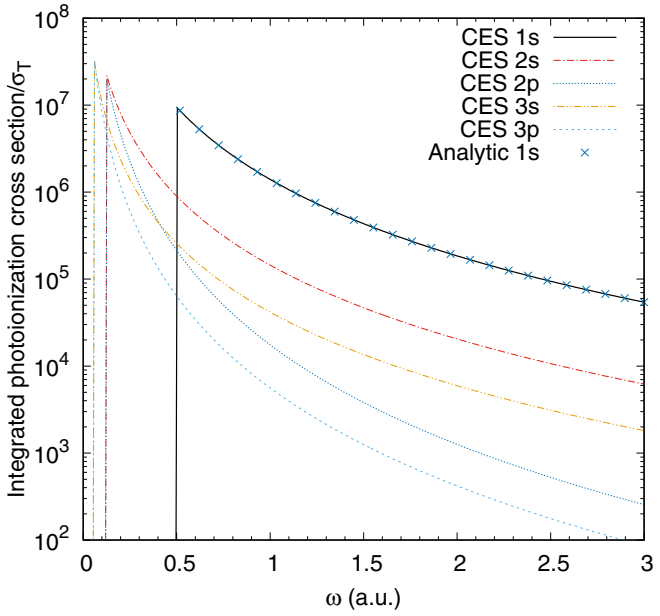

FIG. 7. Photoionization from the first few states of hydrogen using the CES method. Comparison is made to the analytic photoionization cross section from the $1s$ state [18].

For Figs. 4–7 we have only presented the results of the CES method. We also performed calculations using the PV method in Sec. III A and found no difference for all possible cross sections. The ability of the CES method to produce all cross sections presented in this paper within a single calculation shows its efficiency and versatility, while comparison to the PV method allows us to confirm the validity of the cross sections for all cases where analytic results were unavailable.

V. CONCLUSION

We have presented two computational methods for calculation of photon scattering from atomic hydrogen in the nonrelativistic dipole approximation. The PV method involves straightforward evaluation of the KHW matrix element through calculation of a large number of bound eigenstates and generation of continuum eigenstates on an energy grid suitable for calculation of the principal value integral. This method provides a direct computation of the matrix elements and is suitable for testing the validity of our second, more computationally efficient method. The CES method involves calculation of the pseudostates of the complex scaled Hamiltonian in a finite-L^2 basis. It accurately captures the analytic structure of the Green's function and does not require calculation of true bound and continuum eigenstates of the target. This method allows for accurate and efficient calculation of cross sections at any number of energies and with little computational overhead.

We expect that the versatility of the method, combined with the use of finite-L^2 techniques, will allow generalization to more complicated systems and processes. The ability of both the PV and the CES methods to calculate scattering cross sections at energies above the ionization threshold allows calculations in the extreme UV and soft x-ray energy regimes. At such energies the dipole approximation becomes progressively less accurate, and the higher-order terms of the $e^{i\mathbf{k}\cdot\mathbf{r}}$ expansion become relevant. The extension of both methods to account for such terms will be considered elsewhere.

For highly charged hydrogenlike ions relativistic effects become important and, for the photon energies of interest in this work, can well be described by the Dirac equation [32]. The PV and CES methods developed here allow for a straightforward generalization to the relativistic case. For the PV method the exact bound and continuum states of the Dirac-Coulomb Hamiltonian are available. Complex scaling methods have already been applied to study resonances in Dirac Hamiltonians [33,34], and so for the CES method we can utilize the Dirac L spinors in exactly the same way as done in the relativistic formulation of the convergent close-coupling method [35].

ACKNOWLEDGMENTS

This work was supported by the United States Air Force Office of Scientific Research, Curtin University, and resources provided by the Pawsey Supercomputing Centre with funding from the Australian Government and the Government of Western Australia.

APPENDIX A: RAMAN 1*s*-2*s* ANALYTIC CALCULATIONS

Saslow and Mills [10] presented the analytic form of the scattering matrix element for $1s \rightarrow 2s$ photon scattering transitions. Their reduced matrix element M is related to our form of the scattering tensor by

$$M = \frac{\omega\omega'}{\sqrt{3}} A^{(0)*}_{2s,1s}, \tag{A1}$$

which allows for comparison of our numerical calculations to their analytic results. Correcting a typo in [10], we note that the full contribution from the continuum is given by

$$M^{(c)} = -\frac{512\sqrt{2}}{3}\int_0^\infty dn \frac{n^3 \exp\left[-2n\arctan(1/n) - 2n\arctan(2/n)\right]}{(n^2+1)(n^2+4)^2(1-\exp[-2\pi n])}\left(\frac{1}{1+\frac{1}{n^2}-r+i0} + \frac{1}{\frac{1}{4}+\frac{1}{n^2}+r}\right). \tag{A2}$$

The pole term occurs at $n' = (r-1)^{-1/2}$. The form for the imaginary contribution by the continuum is then

$$\mathrm{Im}\{M^{(c)}\} = \frac{512\sqrt{2}}{6}\frac{\pi n'^6 \exp[-2n'\arctan(1/n') - 2n'\arctan(2/n')]}{(n'^2+1)(n'^2+4)^2(1-\exp[-2\pi n'])}. \tag{A3}$$

APPENDIX B: VELOCITY FORM

If we consider the KHW matrix given in Eq. (3) in the dipole approximation, we have

$$M_{fi} = \boldsymbol{\epsilon}\cdot\boldsymbol{\epsilon}'^*\langle f|i\rangle - \sum\!\!\!\!\!\!\int_t \left[\frac{\langle f|\boldsymbol{\epsilon}'^*\cdot\mathbf{p}|t\rangle\langle t|\boldsymbol{\epsilon}\cdot\mathbf{p}|i\rangle}{E_{n_t l_t} - E_{nl} - \omega - i0} + \frac{\langle f|\boldsymbol{\epsilon}\cdot\mathbf{p}|t\rangle\langle t|\boldsymbol{\epsilon}'^*\cdot\mathbf{p}|i\rangle}{E_{n_t l_t} - E_{nl} + \omega'}\right]. \tag{B1}$$

It is useful to compare our calculations in the length gauge to those in the velocity gauge. The two forms are equivalent only when the complete set of intermediate states is used, and so comparison between the two forms allows us to check the stability and accuracy of our results. Bassani *et al.* [36] showed that the length form converges more rapidly when the true bound and continuum states are used for calculation of the $1s \rightarrow 2s$ two-photon transition rate, and thus for approximate calculations where the complete set of states is not known the length form is expected to be more accurate.

We first note that if we are considering Raman scattering, i.e., $i \neq f$, then we may follow the same arguments used in taking Eq. (4) to Eq. (8) to write the total integrated unpolarized cross section as

$$\sigma_{n'l'nl} = \sigma_T \frac{\omega'}{\omega}\frac{1}{3(2l+1)}\sum_\kappa (2\kappa+1)\left|B^{(\kappa)}_{n'l'nl}\right|^2, \tag{B2}$$

where

$$B^{(\kappa)}_{n'l'nl} = (-1)^{l+l'+\kappa}\sum\!\!\!\!\!\!\int_t \begin{Bmatrix} l & l' & \kappa \\ 1 & 1 & l_t \end{Bmatrix}\langle n'l'\|p\|n_t l_t\rangle\langle n_t l_t\|p\|nl\rangle\left[\frac{1}{E_{n_t l_t} - E_{nl} - \omega - i0} + \frac{(-1)^\kappa}{E_{n_t l_t} - E_{nl} + \omega'}\right]. \tag{B3}$$

If we are considering Rayleigh scattering, then taking into account the $\langle f|i\rangle$ term gives

$$\sigma_{nlnl} = \sigma_T\left[1 + \frac{2}{\sqrt{3(2l+1)}}\mathrm{Re}\left\{B^{(0)}_{nlnl}\right\} + \frac{1}{3(2l+1)}\sum_\kappa (2\kappa+1)\left|B^{(\kappa)}_{nlnl}\right|^2\right]. \tag{B4}$$

Finally, similarly to Eq. (9) the polarizability may be given by

$$B^{(0)}_{nlnl} = \sqrt{3(2l+1)}\omega^2\alpha(\omega), \tag{B5}$$

giving the photoionization cross section as

$$\sigma^I_{nl} = \sigma_T\frac{c^3}{2\omega}\mathrm{Im}\left\{B^{(0)*}_{nlnl}\right\}\sqrt{\frac{3}{2l+1}}. \tag{B6}$$

APPENDIX C: CES VELOCITY FORM

We may follow the same arguments given in Sec. III B to apply the complex exterior scaling method to calculation of the terms $B^{(\kappa)}_{n'l'nl}$. In this case the terms are found using

$$B^{(\kappa)}_{n'l'nl} = \theta(-1)^{l+\kappa+1}\sum_t \begin{Bmatrix} l & l' & \kappa \\ 1 & 1 & l_n \end{Bmatrix}\left(\psi_{n'l'}\|\nabla\|\chi^\theta_{n_t l_t}\right)_\theta\left(\psi_{nl}\|\nabla\|\chi^\theta_{n_t l_t}\right)_\theta\left[\frac{1}{W_{n_t l_t} - E_{nl} - \omega} + \frac{(-1)^\kappa}{W_{n_t l_t} - E_{nl} + \omega'}\right], \tag{C1}$$

where

$$\left(\psi_{nl}\|\nabla\|\chi^{\theta}_{n_t l_t}\right)_{\theta} = \frac{(-1)^l}{\theta}\sqrt{(2l+1)(2l_t+1)}\begin{pmatrix} l & 1 & l_t \\ 0 & 0 & 0 \end{pmatrix}\left[\int dr\, u_{nl}(r\theta)\left(\frac{d}{dr}+\frac{c_{l,l_t}}{r}\right)v^{\theta}_{n_t l_t}(r)\right] \tag{C2}$$

and

$$c_{l,l'} = \frac{l'(l'+1)-l(l+1)}{2}. \tag{C3}$$

For all scattering transitions presented in this paper we produced the cross sections using both the length and the velocity forms of the CES method and found that the two forms were essentially indistinguishable.

[1] H. A. Kramers and W. Heisenberg, Z. Phys. **31**, 681 (1925).
[2] I. Waller, Z. Phys. **58**, 75 (1929).
[3] J. Sakurai, *Advanced Quantum Mechanics* (Addison-Wesley, Reading, MA, 1967).
[4] J. H. Ferraro, K. Nakamoto, and C. W. Brown, *Introductory Raman Spectroscopy* (Academic Press, New York, 2003).
[5] D. H. Sampson, ApJ **129**, 734 (1959).
[6] W. F. Huebner and W. D. Barfield, *Opacity* (Springer-Verlag, New York, 2014).
[7] S. Lloyd, Science **321**, 1463 (2008).
[8] M. Lanzagota, *Quantum Radar* (Morgan & Claypool, Williston, VT, 2012).
[9] M. Gavrila, Phys. Rev. **163**, 147 (1967).
[10] W. M. Saslow and D. L. Mills, Phys. Rev. **187**, 1025 (1969).
[11] H. R. Sadeghpour and A. Dalgarno, J. Phys. B **25**, 4801 (1992).
[12] K. Drühl, Phys. Rev. A **26**, 863 (1982).
[13] A. Delserieys, F. Y. Khattak, S. Sahoo, G. F. Gribakin, C. L. S. Lewis, and D. Riley, Phys. Rev. A **78**, 055404 (2008).
[14] H. Bachau, M. Dondera, V. Florescu, and T. A. Marian, J. Phys. B **50**, 174003 (2017).
[15] M. Dondera, V. Florescu, and H. Bachau, Phys. Rev. A **95**, 023417 (2017).
[16] E. Balslev and J. M. Combes, Commun. Math. Phys. **22**, 280 (1971).
[17] B. Simon, Commun. Math. Phys. **27**, 1 (1972).
[18] T. N. Rescigno and V. McKoy, Phys. Rev. A **12**, 522 (1975).
[19] L. D. Landau and E. M. Lifshitz, *Relativistic Quantum Theory*, *Course of Theoretical Physics* (Pergamon Press, Oxford, UK, 1965).
[20] D. A. Varshalovich, A. N. Moskalev, and V. K. Khersonskii, *Quantum Theory of Angular Momentum*, 1st ed. (World Scientific, Philadelphia, 1988).
[21] K. D. Bonin and V. V. Kresin, *Electric-Dipole Polarizabilities of Atoms, Molecules, and Clusters* (World Scientific, Singapore, 1997).
[22] C. M. J. Wijers, Phys. Rev. A **70**, 063807 (2004).
[23] F. H. M. Faisal, *Theory of Multiphoton Processes*, 1st ed. (Springer, New York, 1987).
[24] I. Bray and A. T. Stelbovics, Phys. Rev. A **46**, 6995 (1992).
[25] I. Bray, D. V. Fursa, A. S. Kheifets, and A. T. Stelbovics, J. Phys. B: At. Mol. Opt. Phys. **35**, R117 (2002).
[26] M. C. Zammit, D. V. Fursa, J. S. Savage, and I. Bray, J. Phys. B: At. Mol. Opt. Phys. **50**, 123001 (2017).
[27] S. Han and D. R. Yarkony, Mol. Phys. **110**, 845 (2012).
[28] N. Moiseyev, P. Certain, and F. Weinhold, Mol. Phys. **36**, 1613 (1978).
[29] B. Giraud and K. Katō, Ann. Phys. **308**, 115 (2003).
[30] E. Anderson, Z. Bai, C. Bischof, J. Demmel, J. Dongarra, J. D. Croz, A. Greenbaum, S. Hammarling, A. McKenney, S. Ostrouchov *et al.*, *LAPACK Users's Guide* (Society for Industrial and Applied Mathematics, Philadelphia, PA, 1992).
[31] V. Florescu and A. Cionga, Z. Phys. A **321**, 187 (1985).
[32] T. Jahrsetz, S. Fritzsche, and A. Surzhykov, Phys. Rev. A **89**, 042501 (2014).
[33] P. Šeba, Lett. Math. Phys. **16**, 51 (1988).
[34] A. D. Alhaidari, Phys. Rev. A **75**, 042707 (2007).
[35] D. V. Fursa and I. Bray, Phys. Rev. Lett. **100**, 113201 (2008).
[36] F. Bassani, J. J. Forney, and A. Quattropani, Phys. Rev. Lett. **39**, 1070 (1977).